Composites: Part A 167 (2023) 107404

Contents lists available at ScienceDirect

Composites Part A

journal homepage: www.elsevier.com/locate/compositesa

New approach for electric vehicle composite battery housings: Electromagnetic shielding and flame retardancy of PUR/UP-based sheet moulding compound

Carl-Christoph Höhne *, Philipp Blaess, Sergej Ilinzeer, Patrick Griesbaum

Fraunhofer Institute for Chemical Technology ICT, Joseph-von-Fraunhofer Str. 7, 76327 Pfinztal, Germany

ARTICLE INFO

Keywords:
A: Multifunctional composites
A: Thermosetting resin
B: Flame/fire retardancy
B: Electrical properties

ABSTRACT

In a battery electric vehicle, the battery housing fulfils safety functions such as electromagnetic shielding and flame retardancy. Composites like sheet moulding compounds (SMCs) offer significant potential in the production of battery housings. However, to achieve both electromagnetic shielding and flame retardancy in one material, conventional SMCs must be modified. This study examined the electromagnetic shielding and flame retardancy of unsaturated polyester polyurethane hybrid (UPPH) resin-based SMCs containing either glass- or carbon-fibre reinforcement as well as carbon black, carbon nanotubes, carbon nanostructures or expandable graphite filler. The electromagnetic shielding was tested using test plates and test housings. The flame retardancy was investigated by limiting oxygen index (LOI) tests, UL94 tests, cone calorimeter tests and bench-scale fuel fire tests. The best results in terms of electromagnetic shielding and flame retardancy were achieved by using UPPH composites with 50 wt-% carbon fibres and 11.5 wt-% expandable graphite.

1. Introduction

The automotive industry is currently in a transition phase, facing a massive shift from fossil-fuel-based vehicles towards electro mobility. Aiming for a greener transportation and mobility sector, with the reduction of both greenhouse gas emissions and the dependency on fossil fuels, the trend towards electrified driving will only increase in the future. In this context, battery electric vehicles (BEVs) have shown increasing popularity and prevalence in recent years [1].

The battery of such vehicles is currently the subject of intensive research and development activities. Improvements of the battery capacity as well as the battery charging speed are necessary to increase the vehicle's range and to achieve similar levels of flexibility as conventional internal combustion engine vehicles. However, this often comes with the cost of increasing battery (and therefore car) weight. Current BEV models are usually significantly heavier than their counterparts with an internal combustion engine [2]. Thus, light weighting remains an important factor in vehicle design. For this purpose, composite materials offer excellent weight specific mechanical performance, well suited for most structural applications in the automotive sector. Composite-based battery housing solutions in particular have recently seen a great deal of interest. Compared to state-of-the-art metal-based housings, they exhibit greater weight-saving potential, superior corrosion resistance and thermal insulation, and various other benefits [3–5]. Sheet moulding compound (SMC), and carbon-fibre-reinforced SMC (SMC-CF) in particular, is especially suitable for this application. SMC-CF combines a good weight-specific mechanical performance with a high degree of design freedom of parts, as well as high productivity and cost efficiency. The capability of SMC for hybridization and functional integration further increases its lightweight potential by reducing the number of components necessary.

The composite housing needs to protect the electronics and battery cells reliably from outside influences, i.e. from physical impacts and environmental influences such as temperature and electromagnetic interferences (EMI). In regards to structural performance, SMC-CF should withstand any relevant mechanical load, as shown by Coren et al. [6] in a design study of a battery housing with integrated thermal management. Both structural and crash performance were investigated. Concerning flame resistance of SMC, there are concepts using either inherently flame-resistant resin systems such as phenolic [7], or incorporating flame-retardant additives or fillers in the SMC formulation to achieve the required flammability resistance [8].

There is, however, a lack of literature when it comes to the EMI shielding properties of SMC-based parts. Metal-based housings exhibit

* Corresponding author.
E-mail address: carl-christoph.hoehne@ict.fraunhofer.de (C.-C. Höhne).

https://doi.org/10.1016/j.compositesa.2022.107404
Received 25 July 2022; Received in revised form 18 December 2022; Accepted 22 December 2022
Available online 24 December 2022

excellent shielding efficiency due to their high conductivity and permeability, especially when compared directly to conventional polymers, which are inherently non-conductive. However, metals face issues regarding corrosion. They also have limited lightweight potential compared to composites [9,4]. Shielding in polymer composites is achievable by either using intrinsically conductive polymers [10–12], applying a conductive coating to the composite surface, or by using conductive or magnetic filler materials in the bulk polymer [9]. The latter approach is most attractive for high-volume SMC applications for reasons of general feasibility, productivity, material cost and process efficiency. A great variety of filler types for shielding purposes exists. They can be generally subdivided into carbon-based filers, such as carbon nanotubes (CNT) [13–15] or carbon black [16,17], carbide-based fillers, oxides and ferrites [18–20], as well as sulphides [21,18]. Carbon-based fillers are especially suitable for lightweight applications due to their low density and high surface-to-weight ratio. They exhibit excellent conductivity, which benefits shielding efficiency. Their non-magnetic nature might, however, lead to poor magnetic shielding [21]. On the processing side, the filler-induced viscosity increase might significantly limit processing options, especially when a high filler amount is necessary to reach the percolation threshold [4]. The aim of this study was to investigate the electromagnetic shielding and flame resistance properties of a SMC based on an unsaturated polyester-polyurethane hybrid resin system [22,23]. Different types of filler materials in varying concentrations were incorporated into the resin paste. SMC with either glass- or carbon-fibre reinforcement was investigated. However, the effects of fibre type, fibre length, fibre volume fraction, etc. were not investigated and will form part of further studies. The results are detailed in the following sections.

2. Experimental part

2.1. Materials

Composite materials for the experimental investigations performed in this work were produced at Fraunhofer ICT, Pfinztal, Germany, starting with the production of the semi-finished materials to the compression moulding of SMC plates and parts. The base materials used are detailed in the following.

The Daron UPPH resin system from AOC, Schaffenhausen, Switzerland is the backbone of each formulation produced. Glass fibre reinforced material variants are based on the resin system Daron ZW 14141, while for carbon fibre reinforced material variants, the resin Daron 8151 was used. The resins differ mainly in initial viscosity, with the latter being of lower viscosity for improved impregnation quality in high fibre content SMC-CF applications. The process additives used in the formulations and their respective function are: Internal release agent: BYK 9085 from BYK, Wesel, Germany; Defoamer and air release agent: BYK 9085 from BYK, Wesel, Germany; Inhibitor: 10 % pBQ in MMA form Sigma Aldrich now Merck, Darmstadt, Germany, Initiator: Trigonox 117 from Nouryon, Köln, Germany; Isocyanate: Lupranat M20R from BASF, Ludwigshafen, Germany. With the Daron resin system, isocyanate is used as thickening agent instead of commonly used magnesium oxide.

Two fibre types were used, Multistar 272 4800 60 E-glass fibres (GF) form Johns Manville, Denver, USA with 4800 tex, and PX35-05015 W-13 carbon fibres (CF) from Zoltek, with 50 K tow size, tensile strength of 4,137 MPa, a tensile modulus of 242 GPa, an electrical resistivity of 0.00155 Ω•cm, a fibre diameter 7.1 μm, and a density of 1.81 g/cm^3.

For electromagnetic shielding and flame retardancy functionalization, the following additives were investigated: Expandable graphite (EG): GHL PX90/-2 with a D50 of approx. 40–70 μm from Georg H. Luh GmbH, Walluf, Germany, extra conductive carbon black (ECB): Printex XE2 B with a BET surface area of 1000 m^2/g and an average primary particle size of 30 nm from Orion Engineering Carbon, Frankfurt am Main, Germany, multiwall carbon nanotubes (CNT): NC7000 with an average diameter of 9.5 nm, an average length of 1.5 μm and a surface area of 250–300 m^2/g from Nanocyl, Sambreville, Belgium, carbon nanostructures (CNS): PU encapsulated flakes with an average length of 50–90 μm, a thickness of 10 μm, a sizing content of 3–5 % and a bulk density of 0.110–0.160 g/cm^3 from Applied NanoStructured Solutions, Baltimore, USA.

The material variants investigated in this work are summarized in Table 1 and Table 2. With the incorporation of the additives, the formation of a continuous electrically conductive network within the material is targeted. To ensure that the percolation threshold is exceeded, multiple additive content levels were studied for each variant. Since different additive types have different particle shapes and sizes, and thus differing processing characteristics, the amount added to the composite was adjusted for each additive type. Investigations with nanoparticles in form of CNT have shown that processing epoxy resin with a filler content of 1.5 wt-% and higher is difficult due to a high increase in viscosity.[24] Based on these results, the nanoparticles were added in increments of 0.5 wt-% with a maximum of 1.5 wt-%. For ECB and EG, the filler contents were selected in such a way that the incorporation of curing agent and production by the SMC process were still feasible. Higher filler contents were not processable under standard conditions. In addition, the mechanical properties become worse with higher filler content.[25] For the flame retardancy characterization, only the test results of the most promising material modifications with the highest processable additive content are reported.

2.1.1. SMC production

SMC material variants were produced on an HMT 800 SMC line from Schmidt & Heinzmann, Bruchsal, Germany. The target fibre content was 40 wt-% for UPPH-GF and 50 wt-% for UPPH-CF, with a fibre length of 25.4 mm. The resin paste was prepared using a dissolver of type Dispermat LC 400 from VMA Getzmann, Reichshof, Germany. For the preparation of resin pastes with the nanoparticles CNT and CNS, an Exakt 80E three-roll mill from Exakt, Norderstedt, Germany was used since high shear forces are required for sufficient dispersion of the nanoparticles in the resin.[26] The resin pastes with nanoparticles were processes two times with the three-roll mill. The gap widths of the rolls were set to 90 μm and 30 μm. No tempering of the rolls was applied. The fibre incorporation for the material variants with nanoparticles was carried out with a small kneading chamber and a drive from Thermo Fischer Science, Waltham, USA (BMC process).

The mixing order was identical for all formulations, with the isocyanate being added to the mixture last to avoid premature thickening. The produced material was stored at 20 °C for at least three days for maturation.

2.1.2. Preparation of test plates

Compression moulding of sample plates was performed using a Dieffenbacher DYL630/500 hydraulic press from Dieffenbacher, Eppingen, Germany, with parallel motion control and a flat plate mould (cavity dimensions 457 × 457 mm^2). Moulding temperature was 145 °C. A moulding pressure of 10 MPa was applied for 110 s. For SMC charge preparation, the SMC was cut and stacked manually. For each material, stacks with the size of 450 × 450 mm^2 were used, which corresponded to a mould coverage of 96 %. The test plates with the nanoparticles CNT and CNS were produced on a press P 200P/M from Collin, Maitenbeth, Germany, with a flat plate mould (cavity dimensions 100 × 100 mm^2). Moulding temperature was 145 °C and a pressure of 5 MPa was applied for 300 s. The matured resin paste was placed evenly in the cavity (mould coverage of 100 %). The target thickness of the sample plates was 3 mm. The test plate weights and thicknesses are listed in Table 2. The surfaces of the test plates showed a consistently high quality.

2.1.3. Preparation of composite test housings

Composite test housings were produced using the same Dieffenbacher DYL630/500 hydraulic press from Dieffenbacher, Eppingen,

Table 1
Composition of SMC material variants.

#	Additive	Additive content of the SMC part [wt-%]	Additive content of the resin paste [wt-%]	Fibre	Fibre content [wt-%]
UPPH-GF40	–	–		GF	40
UPPH-CF50	–	–		CF	50
UPPH-GF40-CNT0.6	CNT	0.6	1	GF	40
UPPH-CF50-CNT0.5	CNT	0.5	1	CF	50
UPPH-GF40-CNS0.6	CNS	0.6	1	GF	40
UPPH-CF50-CNS0.5	CNS	0.5	1	CF	50
UPPH-GF40-ECB3.6	ECB	3.6	6	GF	40
UPPH-CF50-ECB1.5	ECB	1.5	3	CF	50
UPPH-GF40-EG13.8	EG	13.8	23	GF	40
UPPH-CF50-EG8.5	EG	8.5	17	CF	50
UPPH-CF50-EG10.0	EG	10.0	20	CF	50
UPPH-CF50-EG11.5	EG	11.5	23	CF	50

Table 2
Test sample properties and tests performed for each material variant.

#	**Final parts weight [g]**	**Final part thickness [mm]**	**Magnetic shielding** on plates	**Electric shielding** on plates	**Electro-magnetic shielding** on housing	**Flame retardancy tests** (LOI, UL94, Cone calorimeter, Bench scale fuel fire)
UPPH-GF40	970	3.23 ± 0.1	x			
UPPH-CF50	894	3.1 ± 0.2	x	x	x	x
UPPH-GF40-CNT0.6		3.3 ± 0.0	x			
UPPH-CF50-CNT0.5		3.57 ± 0.1	x	x		
UPPH-GF40-CNS0.6		3.3 ± 0.0	x			
UPPH-CF50-CNS0.5		3.6 ± 0.0	x			
UPPH-GF40-ECB3.6	1000	3.1 ± 0.1	x			
UPPH-CF50-ECB1.5	952	3.1 ± 0.0	x	x		
UPPH-GF40-EG13.8	996	3.0 ± 0.1	x			
UPPH-CF50-EG8.5	936	3.0 ± 0.0	x			x
UPPH-CF50-EG10.0	960	3.0 ± 0.0	x			x
UPPH-CF50-EG11.5	941	2.9 ± 0.1	x	x	x	x
Aluminium plate, 0.1 mm		0.1 ± 0.0	x	x		
Aluminium plate, 1 mm		1.0 ± 0.0	x			
UPPH-CF50-EG11.5 with polished contact area of the box half shells	2201				x	
UPPH-GF40 with aluminium foil cover	2542	4–6 (housing has varying wall thickness)			x	
UPPH-CF50	1902				x	
UPPH-CF50-EG11.5	2170				x	

Germany, and identical process parameters. The initial charge coverage was 95 %. No inserts were used for bolting. The design of the housing was kept simple in the form of a rectangular box made of two half-shells. One individual SMC box, as shown in Fig. 1, was 400 mm in length, 260 mm in width, and 85 mm in height. The box thickness varied from 4 to 5 mm. Holes were drilled in the upper edge of the half shells at a distance of 70 mm. Two of those SMC boxes were joined via screw connection to form the composite test housing for the subsequent characterization. In total, four different part variants were produced: UPPH-GF housing with aluminium film surface cover, UPPH-CF housing with expandable graphite, UPPH-CF housing with expandable graphite and polished surface, and UPPH-CF without any functional filler (reference housing). Material variants were chosen based on the results of the plaque-level investigation of electromagnetic shielding properties. For the UPPH-GF housing with aluminium film, a self-adhesive aluminium foil was used and applied bubble-free with the aid of a spatula. For the UPPH-CF housings, polishing of the contact surfaces of both box half shells was intended to expose the carbon fibres to enable a continuous conductive contact surface. The surface treatment was carried out manually using sandpaper.

Fig. 1. Two halves of the composite test housing made of UPPH-GF40 covered with aluminium foil.

2.2. Characterization

2.2.1. Electromagnetic shielding: characterization of test plates

For a preliminary characterization, a shielding measurement was performed using 80 × 80 mm^2 plates. The test rig shown in Fig. 2

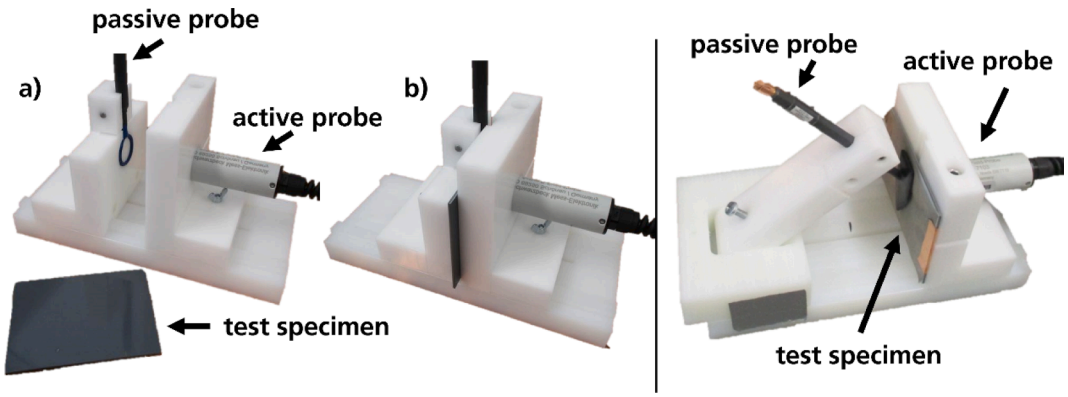

Fig. 2. Left: Test setup for the magnetic near-field shielding measurements: a) test specimen in front of the test setup and b) test specimen installed in the test setup. Right: Test setup for the electric near-field shielding measurements on composite plates.

consisted of two antennas, a passive field probe and an active field probe. The probes were each connected to a Vector Network Analyzer (VNA) from Rohde & Schwarz, München, Germany. The distance between the probes was 10 mm. The plate to be tested was clamped between the two antennas. The passive field probe transmits through the material to the active field probe and the shielding effectiveness is determined using the VNA. With this test setup, the shielding properties in the near field of an electromagnetic transmitter were investigated in the frequency range of 10 kHz to 1 GHz. Two different characterization methods were used: A rod antenna was used to determine the shielding in an electrically dominant near field. The measurement was performed with a passive probe RF-E 02 from Langer, Bannewitz, Germany, and an active probe EFS 7103 from Schwarzbeck Mess-Elektronik, Schönau, Germany. A loop antenna, on the other hand, was used to measure the shielding in a magnetically dominant near field. In order to cover the frequency range from 10 kHz to 1 GHz, two separate measurements were performed. For 10 kHz to 30 MHz, a LF-R 400 from Langer, Bannewitz, Germany, was used as passive probe and a HFSL 7101 from Schwarzbeck Mess-Elektronik, Schönau, Germany, as active probe. For 30 MHz to 1 GHz, a RF-R 400–1 from Langer, Bannewitz, Germany, was used as passive probe and a HFSH 7102 from Schwarzbeck Mess-Elektronik, Schönau, Germany, as active probe.

2.2.2. Electromagnetic shielding: Characterization of a housing

The electromagnetic shielding properties of the composite housings were tested in an anechoic chamber using a 3149 BiConiLog transmitter antenna from ETS Lindgren, Cedar Park, USA, and a dipole that served as a receiver. Both components were connected to a VNA from Rohde & Schwarz, München, Germany. Fig. 3 shows the positions of the antenna and the housing in the anechoic room. The distance between the antenna and the dipole was 1 m. To integrate the dipole into the housing, a hole was drilled in the side wall of the housing and the cable was inserted from the outside using an SMA adapter. A frequency range from 80 MHz up to 1 GHz was investigated. To isolate the shielding effect of the housing, the influence of the absorber hall was determined by reference measurements carried out without a housing. A summary of the selected material combinations and measurements is given in Table 2.

2.2.3. Limiting oxygen index (LOI) test

The LOI value was measured by using an oxygen index module from FIRE, Frankfurt am Main, Germany according to DIN EN ISO 4589–2 standardized procedure. The used sample size was type III (80 × 10 × 1 mm^3).

2.2.4. UL94 test

The UL94 V test was performed with a UL94 Test Device from WAZAU, Berlin, Germany according to the UL94 standard using 13 × 125 × 3 mm^3 samples. In the UL94 test, a 50 W Bunsen burner is applied

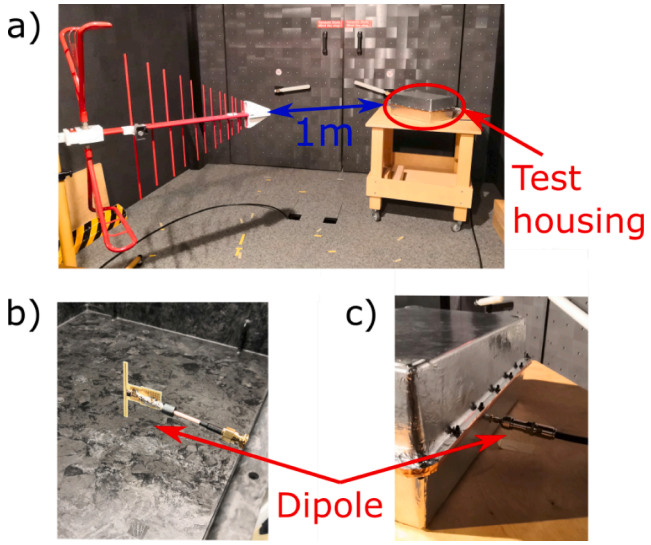

Fig. 3. Test setup for the electromagnetic shielding measurements on test housings. a) Antenna and housing in the anechoic room. b) The dipole used as receiver inside the housing. c) Passage of the cable to the dipole with closed housing.

two times for ten second each on a test specimen.

2.2.5. Cone calorimeter test

Cone calorimeter measurements were taken using an ISO 5660–1 device from WAZAU, Berlin, Germany. The sample size was 100 × 100 mm^3 (thickness depending on plate or sandwich thickness), with three samples tested for each material. The samples were wrapped in aluminium foil and positioned horizontally at a distance of 25 mm from the cone base heater plate, where a heat flux of 35 kW/m^2 was applied. The data were recorded in increments of 1 s.

2.2.6. Bench scale fuel fire test for the UNECE-R100-8E test

A laboratory flammability test stand developed for testing of intumescent coating by Rüttgers Organic GmbH, Mannheim, Germany was modified by using a 170 × 170 mm^2 steel pan filled with 60 mL of petrol (Super 95 E5, DIN EN 228, ROZ 95) to create a fuel fire for about 100–130 s. The distance between steel pan and surface of the test specimen is about 300 mm. 190 × 190 mm^2 test specimens, mounted into a steel test specimen holder, were used. The temperature of the test specimen back side was measured by a surface thermo probe (K type, measurement range −50 °C to +650 °C) from B & B Thermo-Technik, Donaueschingen, Germany and recorded in increments of 1 s.

3. Results and discussion

3.1. Electromagnetic shielding results of test plates

Shielding effectiveness of the magnetic near-field and the electric near-field were measured using GF and CF reinforced UPPH test plates.

3.1.1. Magnetic near-field shielding

Magnetic near-field measurements were performed in the frequency range of 10 kHz to 1 GHz. Fig. 4 shows the magnetic shielding effectiveness of four reference materials, two of which are additive-free fibre-reinforced UPPH specimens, UPPH-GF40 and UPPH-CF50, as well as two aluminium plates with a thickness of 0.1 mm and 1 mm, respectively. Unsurprisingly, the aluminium plates show the best shielding effectiveness, with increasing effectiveness at higher panel thickness. Starting at approx. 1 MHz, the CF reinforced UPPH-CF50 specimen also exhibits shielding. The highest magnetic shielding of UPPH-CF50 is approx. 50 dB at a frequency of 400 MHz. For UPPH-GF40, no magnetic shielding is observed in the entire spectrum of the measurement, which can be attributed to the complete lack of electrical conductivity.

Fig. 5 shows the test results of glass fibre reinforced UPPH-GF specimens with various additives at the highest processable additive content, respectively. However, no significant magnetic near-field shielding was observed in any of the specimens. Only UPPH-GF40-CNS0.6 with a CNS content of 0.6 wt-% shows a minimal shielding effect of 9 dB starting at 1 GHz. It is assumed that the additive content was insufficient. The percolation threshold was likely not reached, and no continuous electrically conductive network was formed at the additive content levels investigated. Higher additive content might be necessary for increasing the shielding effect. However, those could not be achieved due to the resulting increase in resin paste viscosity. It was also found that the mechanical strength and stiffness of the produced specimens drop significantly with increasing additive content [25]. GF reinforced UPPH-SMC with electromagnetic shielding properties could therefore not be produced with the approach used.

Magnetic near-field shielding effectiveness of the carbon fibre reinforced UPPH-CF specimens with different additives are displayed in Fig. 6, and compared to the corresponding UPPH-CF50 reference without any additives as well as the aluminium plates. Below 1 MHz, none of the composite specimens show any significant shielding. Therefore, it can be assumed that UPPH-CF50 cannot be functionalized to provide shielding against low-frequency (<1 MHz) magnetic fields with any of the additives investigated. This was to be expected, as the additives used exhibit good electrical conductivity, but poor permeability. A high permeability is required for shielding low-frequency magnetic fields [27,21].

In the frequency range of 1 MHz to 1 GHz, the UPPH-CF50 composites containing additives show an increase in the magnetic near-field

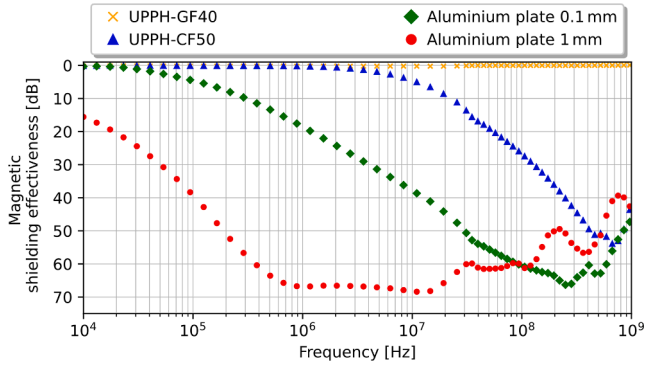

Fig. 4. Magnetic near-field shielding effectiveness of UPPH-GF40, UPPH-CF50 and two aluminium plates. The results were smoothed using a Savitzy-Golay filter with a second-degree polynomial and a grid point interval of 41.

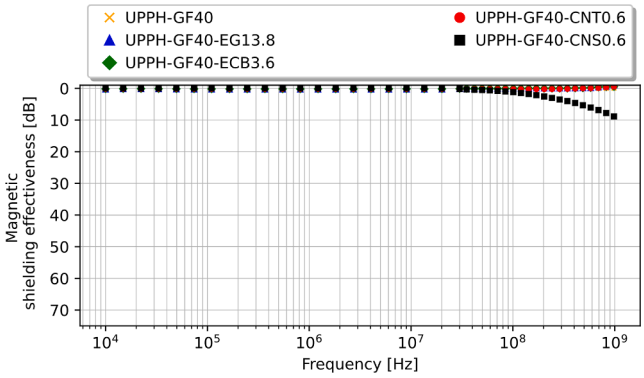

Fig. 5. Magnetic near-field shielding effectiveness of UPPH-GF test plates containing EG, ECB, CNT, and CNS. The results were smoothed using a Savitzy-Golay filter with a second-degree polynomial and a grid point interval of 41.

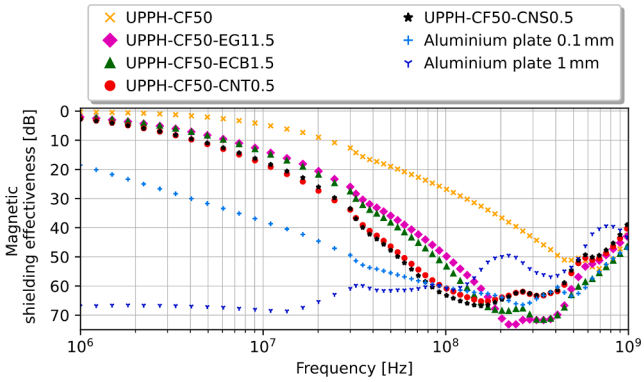

Fig. 6. Magnetic near-field shielding effectiveness of UPPH-CF50 plates containing EG, ECB, CNT, and CNS. The results were smoothed by Savitzy-Golay filter using second-degree polynomial and a grid point interval of 41.

shielding properties in comparison to the UPPH-CF50 reference. In general, all four additive types improve the shielding effectiveness. They also shift the starting point of the effective shielding towards lower frequencies.

Based on the similarity of the measured curves, the material variants with 0.5 wt-% CNS and 0.5 wt-% CNT and the ones with 1.5 wt-% ECB and 11.5 wt-% EG can be grouped, respectively. In direct comparison between those two groups, UPPH-CF50 specimens with CNS / CNT exhibit superior shielding at lower frequencies, especially between 30 and 150 MHz. UPPH-CF50 specimens containing ECB or EG generally show higher shielding in the area of 200 MHz to 1 GHz, especially between 200 MHz and 500 MHz.

The highest magnetic shielding effectiveness of UPPH-CF, which is 53 dB at 400 MHz, is increased to 77 dB at 225 MHz through the addition of 11.5 wt-% EG (UPPH-CF50-EG11.5).

UPPH-CF50 containing CNT or CNS show similar magnetic near-field shielding properties as aluminium in the range of 80 MHz to 1 GHz, and EG or ECB containing UPPH-CF50 in the range of 150 MHz to 1 GHz.

Due to the fact that the expandable graphite-containing specimen variant showed the comparatively best shielding and is not only much more cost-efficient than CNT and CNS, but also provides flame retardant properties, additional specimens of UPPH-CF50 with an overall EG content of 8.5 wt-%, 10 wt-% and 11.5 wt-% were further studied. The magnetic near-field shielding effectiveness is shown in Fig. 7. UPPH-CF50 containing 8.5 wt-% EG and 10 wt-% EG show minimal shielding improvement. However, UPPH-CF50 containing 11.5 wt-% EG shows significant improvement. It is assumed that at a content of 11.5 wt-% EG percolation threshold was surpassed. A maximum electric near-field shielding effectiveness of 77 dB at 225 MHz is observed.

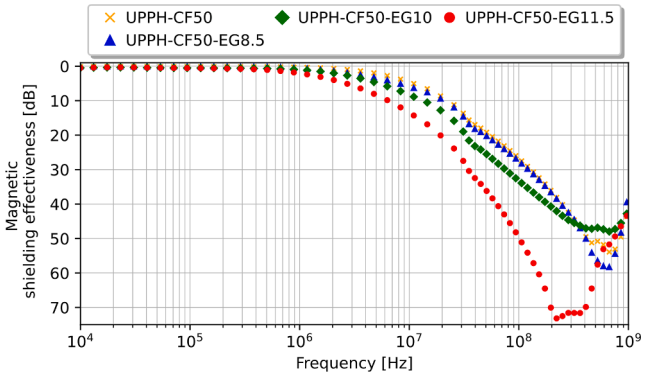

Fig. 7. Magnetic near-field shielding effectiveness of UPPH-CF50 containing different EG contents. The results were smoothed by Savitzy-Golay filter using second-degree polynomial and a grid point interval of 41.

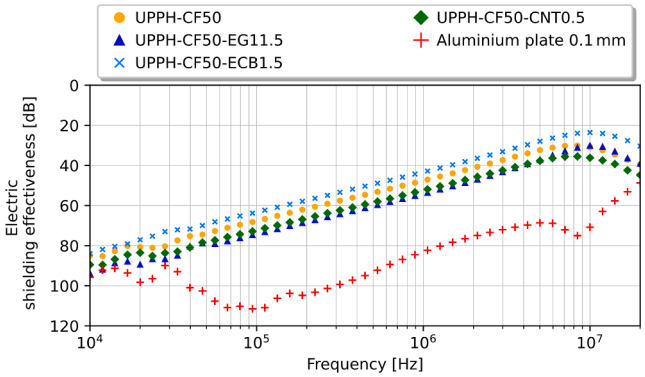

Fig. 9. Electric near-field shielding effectiveness of UPPH-CF50 containing CNT, ECB, and EG. The results were smoothed by Savitzy-Golay filter using second-degree polynomial and a grid point interval of 41.

3.1.2. *Electric near-field shielding*

As UPPH-GF40 composites show very weak to no magnetic near-field shielding, only the electric near-field shielding properties of UPPH-CF50 composites were studied. All tests were carried out in the frequency range from 10 kHz to 1 GHz. However, due to resonance phenomena in the test rig, an interpretation of the test results is only possible up to 10 MHz. Fig. 8 shows the electric near-field shielding effectiveness of UPPH-CF50 and an aluminium plate. As expected, a continuous aluminium layer provides high shielding against low-frequency electric fields. Even a thin aluminium layer of 0.1 mm is sufficient to achieve very high shielding of up to 110 dB. UPPH-CF50 with 50 wt-% CF will provide shielding of 87 dB at 10 kHz. However, the electric shielding effectiveness of UPPH-CF50 decreases continuously with increasing frequency.

To improve the electric near-field shielding of UPPH-CF50, composites containing overall 0.5 wt-% CNT, 1.5 wt-% ECB and 11.5 wt-% EG were studied, see Fig. 9. For UPPH-CF50 containing ECB an overall decrease of the electric shielding effectiveness was observed. For UPPH-CF50 containing CNT and EG an overall increase of the electric shielding effectiveness of about 5 dB was measured.

3.2. *Flame retardancy*

Based on the EMV results, the flame retardancy of UPPH-CF50 composites containing 8.5 wt-% EG, 10.0 wt-% EG and 11.5 wt-% EG were studied by LOI, UL94, Cone Calorimetry tests and a newly developed Bench Scale Fuel Fire test simulating the UNECE-R100-8E test on component level.

The LOI test results are shown in Table 3. Compared to the LOI value of 28.9 O_2% of the EG-free UPPH-CF50, the LOI values slightly increase

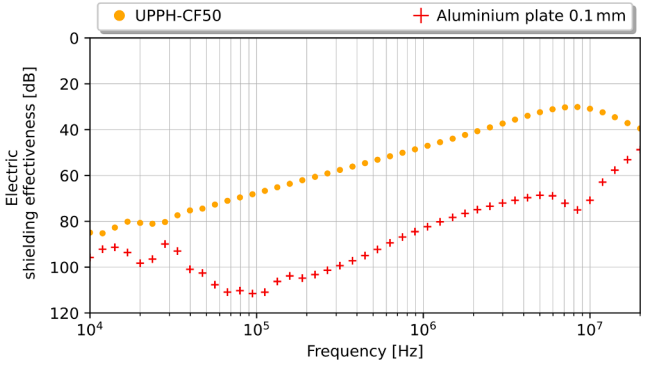

Fig. 8. Electric near-field shielding effectiveness of UPPH-CF50 and aluminium plates. The results were smoothed by Savitzy-Golay filter using second-degree polynomial and a grid point interval of 41.

Table 3
LOI test results of UPPH-CF50 containing EG.

#	FR	FR content [wt-%]	LOI [O_2%]
UPPH-CF50	–	–	28.9 ± 0.38
UPPH-CF50-EG8.5	EG	8.5	28.8 ± 0.52
UPPH-CF50-EG10	EG	10.0	31.3 ± 0.27
UPPH-CF50-EG11.5	EG	11.5	29.1 ± 1.02

for UPPH-CF50 containing 10 wt-% EG and 11.5 wt-% EG. It is assumed that the flame-retardant effect of EG, which is mainly the formation of a thermal protection layer on the fire treated surface, does not significantly influence the burning scenario of the LOI test. Within the LOI test, material ignition and self-extinguishing effect of the material after ignition with a small heat source are tested. A high amount of EG reduces the amount of material which can be pyrolyzed by releasing flammable compounds. The effects of continuing thermal treatment of an external heat source and flame-retardant effects protecting the material from this thermal treatment are not reflected by the LOI test. Therefore, the LOI test results of UPPH-CF50 and UPPH-CF50 containing EG show no differences apart from UPPH-CF50 containing 10 wt-% EG which shows a slightly higher flame retardancy. The higher standard deviation of UPPH-CF50-EG11.5 is attributed to flame retardant effects of EG which leads to the formation of loose char.

Table 4 shows the UL94 test results. UPPH-CF50 without EG as well as UPPH-CF50 containing 8.5 wt-% EG reach no UL94 classification due to strong burning. For both materials, the test specimens burn completely after the second flame treatment. UPPH-CF50 containing 10 wt-% EG is classified as V-1 and UPPH-CF50 containing 11.5 wt-% EG as V-0 a clear V-0 with low afterflame time.

It is assumed that both the reduction of the material which is able to release flammable gases and the formation of a protective char layer by the EG leads to an increased flame retardancy of EG-containing UPPH-CF50. In contrast to the LOI test, a clearly beneficial flame-retardant effect of EG in UPPH-CF50-EG11.5 is observed by the UL94 test.

The test results of the cone calorimetry measurements are shown in Table 5 and the curve of the heat release rate (HRR) is shown in Fig. 10. In comparison, all three UPPH-CF50-EG materials containing EG show similar cone calorimetry test results. However, in comparison with the EG-free UPPH-CF50 a significant improvement of the flame retardancy by the incorporation of EG is observed. Compared to UPPH-CF50, UPPH-CF50-EG11.5 shows a reduction of 67 % for the peak heat release rate (pHRR), a reduction of 33 % for the total heat release (THR) and a reduction of 68 % for the total smoke release (TSR). EG-containing UPPH-CF50 composites show a reduced time to ignition (TTI), an increase of afterflame time and for the residue after 900 s thermal treatment. It is assumed that the formation of a thermally protective char

Table 4
UL94 test results of UPPH-CF50 containing EG.

#	FR content [wt-%]		Afterflame time [s]					Classification
UPPH-CF50	–	1st flame appl.	0	7	0	4	0	No classification
		2nd flame appl.	>30	>30	>30	>30	>30	
UPPH-CF50-EG8.5	8.5	1st flame appl.	0	0	0	0	0	No classification
		2nd flame appl.	16	>30	>30	>30	18	
UPPH-CF50-EG10.0	10.0	1st flame appl.	0	0	0	0	0	V-1
		2nd flame appl.	0	4	0	0	25	
UPPH-CF50-EG11.5	11.5	1st flame appl.	0	0	0	0	0	V-0
		2nd flame appl.	0	0	0	3	5	

Table 5
Cone calorimetry test results of UPPH-CF50 containing EG.

#	TTI [s]	Afterflame [s]	pHRR [kW/m²]	THR [MJ/m²]	TSR [m²/m²]	Residue @900 s [%]
UPPH-CF50	92	486	273	37	1244	54.9
	120	700	240	40	1212	51.2
	105	520	230	39	1301	70.7
	106 ± 14	**569 ± 115**	**248 ± 22**	**39 ± 1.7**	**1252 ± 45**	**59.0 ± 10.4**
UPPH-CF50-EG8.5	68	715	83	22	418	69.0
	90	665	95	29	552	–
	60	646	87	28	579	63.3
	73 ± 16	**675 ± 36**	**88 ± 6**	**27 ± 3.6**	**516 ± 86**	**66.1 ± 4.4**
UPPH-CF50-EG10.0	86	–	87	22	393	72.4
	71	674	101	31	674	62.7
	72	899	86	27	519	69.0
	76 ± 8	**787 ± 159**	**91 ± 8**	**27 ± 4.5**	**528 ± 141**	**68.0 ± 4.9**
UPPH-CF50-EG11.5	82	–	83	26	584	70.2
	95	831	81	24	293	69.1
	71	925	84	28	313	66.1
	83 ± 12	**878 ± 66**	**83 ± 1**	**26 ± 2.3**	**397 ± 163**	**68.5 ± 2.2**

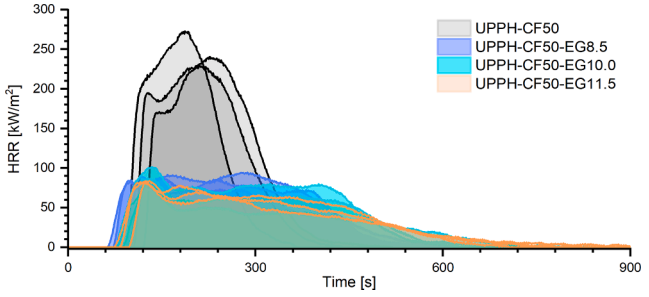

Fig. 10. Heat release rate curve of UPPH-CF50 containing EG.

layer by the EG is responsible for this behaviour. Due to the formation of the char layer, the surface of the test specimen is heated up faster which leads an increase of the pyrolysis rate of the surface and a TTI reduction. However, the inside of the test specimen is protected by the EG-based char leading to significantly reduced pyrolysis rate of the inner polymeric material. Fig. 10 shows the formation of a thermally protective char layer: EG-free UPPH-CF50 shows a single pyrolysis peak with a weak preceding peak of the surface pyrolysis. However, the EG-containing UPPH-CF50 composites show the formation of a heat release plateau which indicate the formation of thermally protective char layer and the gradual release of flammable pyrolysis products form the specimen inside.

To evaluate the burning behaviour of the materials in a more realistic fire scenario, a bench scale fuel fire test with two minutes fuel fire treatment was used. The test results are shown in Table 6 and Fig. 11. Five criteria are used for the test result evaluation:

Self-extinction: All tested specimens are ignited during the flame treatment. However, all specimens of UPPH-CF50 and UPPH-CF50-EG8.5 show self-extinction during the burning time of the fuel fire. UPPH-CF50-EG10.0 shows self-extinction 5 ± 2 s and UPPH-CF50-EG11.5 shows self-extinction 7 ± 7 s after the extinction of the fuel

Table 6
Bench scale fuel fire test results of UPPH-CF50 containing EG.

#	Reverse side ignited	Mass loss [%]	$T_{max,\ reverse\ side}$ [°C]	t of T_{max} [s]
	no	6.8	279.2	120
	no	8.1	283.3	112
	no	6.8	278.2	108
UPPH-CF50	**no**	**7.2 ± 0.76**	**280 ± 2.7**	**113 ± 6.1**
	no	4.6	234.7	114
	no	4.5	237.8	116
	no	4.6	234.7	117
UPPH-CF50-EG8.5	**no**	**4.6 ± 0.03**	**236 ± 1.8**	**116 ± 1.5**
	no	4.7	230.7	108
	no	4.0	237.8	104
	no	3.0	231.7	96
UPPH-CF50-EG10.0	**no**	**3.9 ± 0.88**	**233 ± 3.8**	**103 ± 6.1**
	no	3.8	237.8	112
	no	3.5	236.8	121
	no	5.5	228.6	118
UPPH-CF50-EG11.5	**no**	**4.3 ± 1.11**	**234 ± 5.0**	**117 ± 4.6**

fire. It is assumed that the thermally stable char caused by the EG reduces the pyrolysis rate of the specimens and acts like a candle wick which holds a small flame for a while, which ignites released pyrolysis gases. For a real REESS application, necessary self-extinction properties are fulfilled by all materials. However, the afterburn time of UPPH-CF50-EG10.0 and UPPH-CF50-EG11.5 should be reduced.

Ignition of the reverse side of the specimen: No specimen shows an ignition of the reverse side of the specimen. Accordingly, the flames do not penetrate the specimen. In a real REESS application, an ignition of flammable materials and thermal decomposition products inside des REESS by an external fire is not assumed.

Structural integrity: No specimen shows a loss of structural

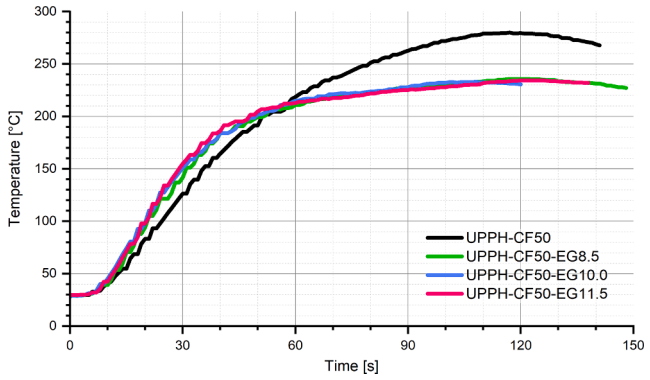

Fig. 11. Temperature profile (mean value) of the specimen back side of UPPH-CF50 containing EG.

integrity. No detaching and falling of material, material deformation or crack formation is observed. The EG containing UPPH-CF50 composites show the formation of porous char on top of the fire treated surface.

Mass loss: The mass loss of UPPH-CF50 is higher than the mass losses of the EG containing composites. The replacement of flammable polymeric materials by EG within the composite as well as the increased formation of char caused by EG is responsible for this.

Temperature of the reverse side of the specimen: The maximum temperature of the reverse side of the specimen ($T_{max,\ reverse\ side}$) is 280 °C for UPPH-CF50 and 233–236 °C for the EG containing composites. The reduction of $T_{max,\ reverse\ side}$ of about 45 °C by the incorporation of EG is an improvement. However, the test criteria of $T_{max,\ reverse\ side} <$ 80 °C (start of the thermal damage of the battery cells) is not fulfilled. In a real REESS application, further technical precautions for example thermal insulation of the battery inside should be implemented.

Overall, the EG containing UPPH-CF50 composites show an improvement compared to the reference composite. However, the inside of the REESS must be designed to handle a 235 °C inside wall temperature.

3.3. Test housings

Based on the test results of the electric and magnetic near-field measurements and the flame retardancy tests, UPPH-CF50-EG11.5 was chosen to build a box-like test housing, see Fig. 12.

Measurements on these test housings provide more insights into the electromagnetic shielding properties of a component like a battery housing. Electromagnetic shielding measurements using plates only provide a statement about the shielding effects of the material itself [28]. However, other factors, such as the geometry of the housing, holes, slots and cable bushings, influence the overall electromagnetic shielding of the housing. These weak points can cancel out the electromagnetic shielding properties of the housing at higher frequencies. Furthermore, these cancelling effects increase with the size, spacing and the number of holes [29].

To test the electromagnetic shielding effectiveness of the studied materials with the test geometry of a battery housing, box-shaped test housings were produced using UPPH-CF50, UPPH-CF50-EG11.5 and UPPH-GF40 reinforced with aluminium foil.

Fig. 13 shows the electromagnetic shielding effectiveness of the three different test housings. All three test housings show similar electromagnetic shielding properties. Compared to UPPH-CF50, the incorporation of 11.5 wt-% EG shows only a small influence on the electromagnetic shielding properties. To improve the magnetic shielding of UPPH-CF50-EG11.5, the contact areas of both box half shells were polished. However, only a small effect was observed. The GF reinforced UPPH-GF40 with aluminium foil cover show slightly worse magnetic shielding than the CF reinforced UPPH-CF50.

Maximum magnetic shielding of 45 dB at 400–425 MHz was achieved by using UPPH-CF50-EG11.5 and of 45 dB at 950 MHz by using UPPH-CF50. However, the design of the test housing has not been investigated or optimised for electromagnetic shielding.

It is assumed that higher electromagnetic shielding effectiveness can be achieved by using an optimized test housing.

4. Conclusions

The electromagnetic shielding and flame retardancy of UPPH composites produced by SMC were studied. On 3 mm test plates, GF-reinforced UPPH shows no electromagnetic shielding. With 50 wt-%, CF-reinforced UPPH shows electromagnetic shielding which can be improved by incorporating CNT, CNS, ECB and EG. The best results in terms of electromagnetic shielding and flame retardancy were achieved by using UPPH composites with 50 wt-% CF and 11.5 wt-% EG. However, for real REESS application, a design which is able to handle high temperatures (235 °C at 3 mm plate level) inside the wall of the REESS housing, in the event of an external fire, should be considered.

Magnetic shielding measurements using box-like test housings show similar shielding properties for UPPH-CF with 50 wt-% CF (with or without 11.5 wt-% EG), and 40 wt-% GF-reinforced UPPH (with an aluminium foil cover).

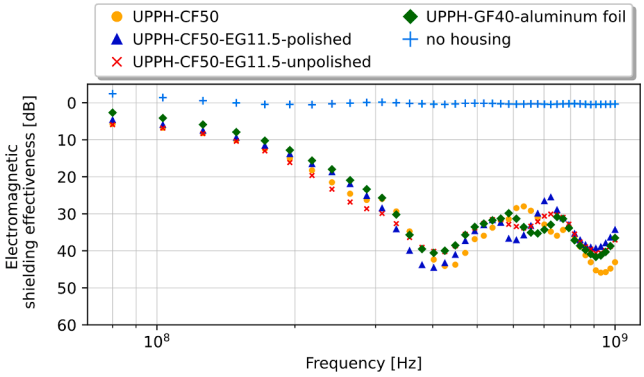

Fig. 13. Eletromagnetic shielding effectiveness of test housings made form UPPH-CF50 containing EG and UPPH-GF40 with aluminium foil cover. The results were smoothed by Savitzy-Golay filter using second-degree polynomial and a grid point interval of 41.

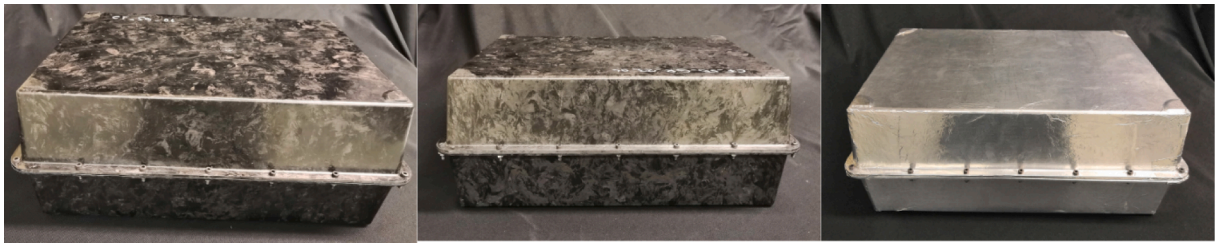

Fig. 12. Box-like test housings made from UPPH-CF50 (left), UPPH-CF50-EG11.5 (middle) and UPPH-GF40 covered with aluminium foil (right).

The test results of electromagnetic shielding using plates allow a first estimation of the electromagnetic shielding behaviour of housings. However, for the same composite the electromagnetic shielding of the test housing is less efficient than the shielding of the plates. It is assumed that weak points of the design of the test housing are responsible for this decrease in electromagnetic shielding effectiveness. To improve shielding, the design of the test housing must be optimized.

CRediT authorship contribution statement

Carl-Christoph Höhne: Conceptualization, Investigation, Writing – original draft, Writing – review & editing. **Philipp Blaess:** Investigation, Writing – original draft, Writing – review & editing. **Sergej Ilinzeer:** Writing – original draft, Writing – review & editing. **Patrick Griesbaum:** Conceptualization, Investigation, Supervision, Project administration, Funding acquisition.

Declaration of Competing Interest

The authors declare that they have no known competing financial interests or personal relationships that could have appeared to influence the work reported in this paper.

Data availability

Data will be made available on request.

Acknowledgements

The authors would like to thank their colleagues from Fraunhofer ICT, Pfinztal: Matthias Stricker, Jürgen Graf for technical and analytical support and the Fraunhofer ICT colleagues from the research group Flame, Fire and Explosion Protection, colleagues from Fraunhofer IISB, Erlangen: Thomas Smazinka for the electromagnetic shielding measurements of the test housings and colleagues from Fraunhofer LBF, Darmstadt: Michael Großhauser and Erik Westphal for the cone calorimetry measurements. Financial support by Ministry of Science, Research and Arts and the Ministry for Economy, Labor and Housing of the state of Baden-Württemberg, as well as through contributions from the Fraunhofer Society, the Hochschule Karlsruhe and the Karlsruhe Institute for Technology in the context of the project Profilregion Mobilitätssysteme Karlsruhe is gratefully acknowledged. All material suppliers are also gratefully acknowledged for providing the materials used.

References

[1] Sanguesa JA, Torres-Sanz V, Garrido P, Martinez FJ, Marquez-Barja JM. A Review on Electric Vehicles: Technologies and Challenges. Smart Cities 2021;4(1):372–404.
[2] Czerwinski F. Current Trends in Automotive Lightweighting Strategies and Materials. Materials (Basel) 2021;14(21).
[3] Schludi C, Joos J. Lightweight and Safe Composite Battery Housings. Lightweight des worldw 2019;12(6):44–7.
[4] Pradhan SS, Unnikrishnan L, Mohanty S, Nayak SK. Thermally Conducting Polymer Composites with EMI Shielding: A review. J Elec Materi 2020;49(3):1749–64.
[5] Wang Z, Käferböck M, Zhao H, Chen H. First Body-in-White Made from Composites for a Chinese Electric Car. ATZ Worldw 2021;123(3):16–21.
[6] Coren F, Huemer-Kals S, Stelzer PS, Fischer P. Crashworthiness of C-SMC: A structural battery case for automotive application. In: FISITA 2020.
[7] Moser L, Heide S, Swentek I, Schmidt U, Seiz M. Thermoset Technologies for Cost Efficient Production of Lightweight Composites. In: Dröder K, Vietor T, editors. Technologies for economic and functional lightweight design. Berlin, Heidelberg: Springer Berlin Heidelberg; 2021. p. 35–41.
[8] Griesbaum P, Höhne C-C, Wall L, Hennin F, Huber T. Investigation of SMC Flame retardants or application in battery electric vehicles. Sampe Europe Conference 2020.
[9] Sathish Kumar K, Rengaraj R, Venkatakrishnan GR, Chandramohan A. Polymeric materials for electromagnetic shielding - A review. Mater Today: Proc 2021;47:4925–8.
[10] Jelmy EJ, Lakshmanan M, Kothurkar NK. Microwave absorbing behavior of glass fiber reinforced MWCNT-PANi/epoxy composite laminates. Mater Today: Proc 2020;26(2–3):36–43.
[11] Jiang D, Murugadoss V, Wang Y, Lin J, Ding T, Wang Z, et al. Electromagnetic Interference Shielding Polymers and Nanocomposites - A Review. Polym Rev 2019;59(2):280–337.
[12] Satheesh Kumar KK, Geetha S, Trivedi DC. Freestanding conducting polyaniline film for the control of electromagnetic radiations. Curr Appl Phys 2005;5(6):603–8.
[13] Hornbostel B, Leute U, Pötschke P, Kotz J, Kornfeld D, Chiu P-W, et al. Attenuation of electromagnetic waves by carbon nanotube composites. Physica E 2008;40(7):2425–9.
[14] Li N, Huang Y, Du F, He X, Lin X, Gao H, et al. Electromagnetic interference (EMI) shielding of single-walled carbon nanotube epoxy composites. Nano Lett 2006;6(6):1141–5.
[15] Singh BP, Prasanta CV, Saini P, Pande S, Singh VN, Mathur RB. Enhanced microwave shielding and mechanical properties of high loading MWCNT–epoxy composites. J Nanopart Res 2013;15(4):1993.
[16] Al-Saleh MH, Sundararaj U. X-band EMI shielding mechanisms and shielding effectiveness of high structure carbon black/polypropylene composites. J Phys D Appl Phys 2013;46(3):35304.
[17] Rahaman M, Chaki TK, Khastgir D. Development of high performance EMI shielding material from EVA, NBR, and their blends: effect of carbon black structure. J Mater Sci 2011;46(11):3989–99.
[18] Garzón Posada AO, Landínez Téllez DA, Roa-Rojas J, Ramos Barrado JR. Electromagnetic shielding response of magnetite elastomeric composites: Source and filler content dependence. J Mater Res Technol 2020;9(5):10597–607.
[19] Tan L, Elnail KEI, Ju M, Huang X. Comparative Analysis and Design of the Shielding Techniques in WPT Systems for Charging EVs. Energies 2019;12(11):2115.
[20] Wang K, Zuo Z, Sang L, Zhu X. Comprehensive Analysis for Electromagnetic Shielding Method Based on Mesh Aluminium Plate for Electric Vehicle Wireless Charging Systems. Energies 2022;15(4):1546.
[21] Liu J, Zhang L, Wu H. Electromagnetic wave-absorbing performance of carbons, carbides, oxides, ferrites and sulfides: review and perspective. J Phys D Appl Phys 2021;54(20):203001.
[22] Bücheler D. Locally Continuous-fiber Reinforced Sheet Molding Compound: Karlsruhe; 2018.
[23] Hohberg M, Kärger L, Bücheler D, Henning F. Rheological In-Mold Measurements and Characterizations of Sheet-Molding-Compound (SMC) Formulations with Different Constitution Properties by Using a Compressible Shell Model. Int Polym Proc 2017;32(5):659–68.
[24] Morais M. Manipulation of carbon nanoparticles in composites with electric fields for improved electrical properties. Karlsruher Institut für Technologie KIT; 2020.
[25] Blaess P. Charakterisierung und Modifizierung der elektromagnetischen Schirmeigenschaften von Sheet Molding Compound. Karlsruher Institut für Technologie; 2021.
[26] Buschhorn ST, Wichmann MHG, Sumfleth J, Schulte K, Pegel S, Kasaliwal GR, et al. Charakterisierung der Dispersionsgüte von Carbon Nanotubes in Polymer-Nanokompositen. Chem Ing Tech 2011;83(6):767–81.
[27] Paul CR. Introduction to electromagnetic compatibility. Hoboken, N.J: Wiley-Interscience; 2006.
[28] Leute U. Kunststoffe und EMV: Elektromagnetische Verträglichkeit mit leitfähigen Kunststoffen; mit 12 Tabellen. Renningen: expert-Verl; 2006.
[29] Wolfsperger HA. Elektromagnetische Schirmung: Theorie und Praxisbeispiele. Berlin, Heidelberg: Springer, Berlin Heidelberg; 2008.